

Positive and Negative Cooperativities at Subsequent Steps of Oxygenation Regulate the Allosteric Behavior of Multistate Sebacylhemoglobin^{†,‡}

Enrico Bucci,^{*,§} Anna Razynska,[§] Herman Kwansa,[§] Zygmunt Gryczynski,[§] John H. Collins,^{||} and Clara Fronticelli[§]

Department of Biological Chemistry, University of Maryland School of Medicine, and Medical Biotechnology Center of the Maryland Biotechnology Institute, University of Maryland, 108 North Greene Street, Baltimore, Maryland 21201

Ron Unger, Michael Braxenthaler, John Moulton, Xinhua Ji, and Gary Gilliland

Center for Advanced Research in Biotechnology of the University of Maryland Biotechnology Institute and National Institute of Standards and Technology, 9600 Gudelsky Drive, Rockville, Maryland 20850

Received October 15, 1995; Revised Manuscript Received December 21, 1995[®]

ABSTRACT: Cross-linked human hemoglobin (HbA) is obtained by reaction with bis(3,5-dibromosalicyl) sebacate. Peptide maps and crystallographic analyses confirm the presence of the 10 carbon atom long sebacyl residue cross-linking the two β 82 lysines of the β -cleft (DecHb). The Adair's constants, obtained from the oxygen binding isotherms, show that at the first step of oxygenation normal hemoglobin and DecHb have a very similar oxygen affinity. In DecHb negative binding cooperativity is present at the second step of oxygenation, which has an affinity 27 times lower than at the first step. Positive cooperativity is present at the third binding step, whose affinity is 380 times that of the second step. The fourth binding step shows a weak negative cooperativity with an affinity one-half that of the third step. Crystals of deoxy-DecHb diffracted to 1.9 Å resolution. The resulting atomic coordinates are very similar to those of Fermi et al. [(1984) *J. Mol. Biol.* 175, 159–174] and Fronticelli et al. [(1994) *J. Biol. Chem.* 269, 23965–23969] for deoxy-HbA. The electron density map of deoxy-DecHb indicates the presence of the 10 carbon bridge between the β 82 lysines. Molecular modeling confirms that insertion of the linker into the T structure requires only slight displacement of the two β 82 lysines. Instead, insertion of the linker into the R and R2 structures [Shaanan (1983) *J. Mol. Biol.* 171, 31–59; Silva et al. (1992) *J. Biol. Chem.* 267, 17248–17256] is hindered by serious sterical restrictions. The linker primarily affects the partially and fully liganded states of hemoglobin. The data suggest in DecHb concerted conformational changes at each step of oxygenation.

For more than 50 years the nonhyperbolic shape of the oxygen binding isotherm of hemoglobin appeared to defy the law of mass action. The puzzle was solved when a third dimension was introduced into the equations describing the fractional saturation of hemoglobin as a function of partial pressure of oxygen. The third dimension was the ligand-linked conformational change of the protein. Two main allosteric models were proposed: the two-state MWC model of Monod et al. (1965) and the multipattern KNF model of Koshland et al. (1966). Other proposed models (DiCera et al., 1987; Gill et al., 1986) are essentially variants of the two basic ones.

The thermodynamics of the two-state MWC model (Monod et al., 1965) assume a system capable of only two conformations, namely, T (low affinity) for the unliganded state and R (high affinity) for the liganded state. In the absence of ligands the equilibrium between the two is defined

by the allosteric constant $L_0 = T_0/R_0$. When L_0 increases, favoring T_0 , the overall oxygen affinity decreases. When R_0 is favored, the oxygen affinity increases. There are no intermediate conformations. The system switches completely from T to R and *vice versa* at a certain step of oxygen saturation which is still not clearly defined. The model cannot explain negative binding cooperativity. It is also inconsistent with the erratic liberation of heat at the subsequent steps of oxygenation found by Bucci et al. (1991) and Johnson et al. (1992). The model, however, remains an effective tool for parametrizing the allosteric regulation of ligand affinity in hemoglobin. This has generated the common perception that allosteric effectors that stabilize the T form lower the oxygen affinity of the system, while if the T form is destabilized, the oxygen affinity increases. Not much regulation is expected from the “relaxed” R form of the system.

The KNF model proposed by Koshland et al. (1966) allows mixed tetramers in which some of the subunits are either in their T or R state. Thus, each intermediate has its own mixed structure. However, each subunit can be only in the T or R conformations. Negative cooperativity occurs when the T–R interactions are stronger than the T–T or R–R interactions. If T–T and R–R interactions prevail, positive cooperativity is produced. The system is still based on two fixed tertiary structures of the subunits: the unliganded T structure and the liganded R conformation.

[†] This work was supported in part by USPHS Grants R01-HL-13164 and P01-HL-48517 and by the computer network of the University of Maryland at Baltimore and at College Park, MD.

[‡] This paper is dedicated to the memory of Jeffries Wyman. He was the first to propose linked functions and conformational changes at the basis of ligand binding cooperativity in macromolecules. He was also a close friend.

[§] Department of Biological Chemistry, University of Maryland School of Medicine.

^{||} Medical Biotechnology Center of the Maryland Biotechnology Institute, University of Maryland.

[®] Abstract published in *Advance ACS Abstracts*, March 1, 1996.

The notion that the hemoglobin system is fully described by one initial and one final configuration has been challenged by the crystallographic description of the R2 (Silva et al., 1992) and Ypsilanti (Smith et al., 1991) hemoglobin structures. They have revealed that liganded hemoglobin has access to additional conformations besides the classic R conformation (Shanaa, 1983). Analysis of the relationship of the known conformations shows that R may be regarded as an intermediate between T and R2 (Srinivasan & Rose, 1994; Janin et al., 1993).

Kluger et al. (1992), Jones et al. (1993), and Bucci and co-workers (Bucci et al., 1994; Bucci & Fronticelli, 1995) have identified several cross-linked hemoglobins with reduced oxygen affinities. These data suggest the relative stabilization of hemoglobin into a lower oxygen affinity conformation as the linker size increases. One of those hemoglobins, cross-linked between the β subunits with the bulky benzenetricarboxylate, shows in the crystal of its oxyform features intermediate between the R and T structures, as in a "nascent R state" (Schumacher et al., 1995). This would be an additional accessible conformation of the liganded state. Thus, it seems likely that other, so far unidentified conformations are on the pathway of the allosteric transition and play a role in determining the allosteric properties of the system.

These structures complicate the R structure concept: which R state is correct and is it unique? Crystal packing, sequence changes, and environmental factors (crystallization solution including pH, ionic strength, organic compounds, etc.) will all influence what is observed in the crystal of liganded hemoglobin.

Continuing these studies, we have investigated the functional and structural characteristics of human hemoglobin intramolecularly cross-linked between the β subunits with the 10 carbon atom long sebacyl residue, DecHb.¹ In terms of p_m 's, the overall oxygen affinity of this compound is approximately twice lower than that of normal hemoglobin. The recovered Adair's parameters indicate that the right shift of the binding isotherm is produced by alternate negative and positive cooperativities of the intermediates of oxygenation, after an initial step identical to that of normal hemoglobin. Crystallographic analyses and molecular modeling indicate that the conformations most likely affected by the cross-link and regulating the allosteric properties of the system are its partially and fully liganded forms.

MATERIALS AND METHODS

Human hemoglobin was prepared and purified as described (Bucci et al., 1988). It was stored at -80°C , after recycling through a mixed-bed resin column to remove all anions and polyanions. Hemoglobin concentration was measured spectrophotometrically using $E = 0.868\text{ cm}^2\text{ mg}^{-1}$ for the carbonmonoxy derivative at 540 nm.

Activation of sebatic acid (DecBDS) was performed as previously described for poly(carboxylic acids) (Razynska et al., 1991). Sebatic acid and 3,5-dibromosalicylate were obtained from Aldrich Chemical Co. The purity of the product was determined by elemental analysis (Atlantic Microlab, Inc.) and by proton NMR spectroscopy. The

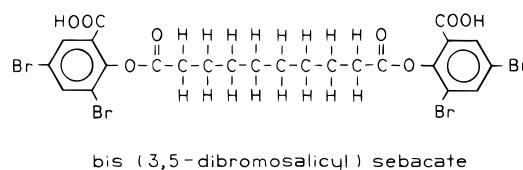


FIGURE 1: Chemical structure of bis(3,5-dibromosalicyl) sebocate.

chemical formula of the bis(3,5-dibromosalicyl) sebocate is shown in Figure 1.

Reaction of Human Hemoglobin with DecBDS. To a 6% solution of deoxygenated hemoglobin in 0.05 M borate buffer at pH 9.0 was added the active form of sebatic acid in a 2:1 to 4:1 molar ratio to tetrameric hemoglobin. The mixture was kept at 37°C for 90 min with continuous stirring, under a stream of nitrogen. We added sodium dithionite (0.5 mg/mL) to ensure the complete deoxygenation of the solutions. The reaction was stopped by the addition of glycylglycine to a final concentration of 0.1 M, followed by dialysis against 0.1 M glycine, in the cold for at least 4 h.

Anion-exchange chromatography was performed on columns packed with DEAE-MCI resin using Waters Delta-Prep 4000 HPLC equipment.² We used gradients formed by 0.015 M Tris-acetate at pH 8.2 and 0.015 M Tris-acetate buffer in 0.2 M sodium acetate at pH 7.4.

Separation of the α and β chains and peptide mapping were performed by reversed-phase chromatography using a C4 Vydac column and a gradient of CH_3CN in 0.1 M TFA. After separation, the β chains were pyridylethylated by classic procedures, equilibrated with 0.1 M bicarbonate, and digested with 1-chloro-3-(tosylamido)-7-amino-2-heptanone-treated trypsin (1:50 w/w) for 20 h at room temperature. The tryptic peptides were separated by HPLC on a Vydac C18 column. Sequences were determined using either an Applied Biosystems Model 477A or a Hewlett-Packard G1000A, following the procedures standardized by the manufacturer.

Sedimentation velocity measurements were performed with a Beckman Model E analytical ultracentrifuge, using the Schlieren optics. The temperature was between 19 and 21°C .

Molecular Modeling. The linker was fitted manually using the modeling package QUANTA running on a 4D-20 Silicon Graphics workstation. The proposed models were checked using the "Protein Health" module of the package to make sure that no geometrical or steric constraints were violated: atoms were not allowed within the van der Waals radius of other atoms, the "trans" conformation of the bond between the C-N of the lysine side chain and the first C-C of the linker was maintained, and the carbon atoms of the linker were not to eclipse each other. Given the present state of the art in numerically based detailed modeling of protein structure (Mosimann et al., 1995), we consider that more elaborate procedures than these would not be informative. Surface areas were calculated using the algorithm of Lee and Richards (1971), with van der Waals radii taken from Chothia (1976). All carbon and sulfur atoms were considered to be nonpolar. It should be noted that the differences

¹ Abbreviations: DecBDS, bis(3,5-dibromosalicyl) sebocate; DecHb, human hemoglobin cross-linked with a sebacyl residue; HbA, human hemoglobin, untreated; p_m = median ligand activity.

² Certain commercial equipment, instruments, and materials are identified in this paper in order to specify the experimental procedure. Such identification does not imply recommendation or endorsement by the National Institute of Standards and Technology, nor does it imply that the material or equipment identified is necessarily the best available for the purpose.

Table 1: Statistical Details of X-ray Diffraction Data Collected for the Cross-Linked Human Deoxyhemoglobin

| shell lower limit (Å) | av intensity I | av $I/s(I)$ | no. of measurements | no. of unique reflections | | | R_w^a | R_{uw}^b |
|--------------------------|------------------|-------------|------------------------|---------------------------|--------|----------------|---------|------------|
| | | | | expected | obsd | $I \geq 2s(I)$ | | |
| 3.45 | 623 | 32.0 | 21 494 | 7 142 | 7 048 | 6 927 | 0.081 | 0.064 |
| 2.74 | 229 | 17.2 | 21 115 | 7 074 | 7 074 | 6 542 | 0.109 | 0.092 |
| 2.39 | 116 | 9.0 | 18 692 | 7 038 | 7 035 | 5 735 | 0.148 | 0.135 |
| 2.17 | 79 | 5.6 | 17 084 | 7 020 | 7 019 | 4 931 | 0.188 | 0.175 |
| 2.02 | 51 | 3.3 | 15 823 | 7 044 | 7 037 | 3 905 | 0.247 | 0.236 |
| 1.90 | 30 | 1.9 | 14 655 | 6 999 | 6 954 | 2 625 | 0.333 | 0.320 |
| totals | 188 | 11.5 | 108 860 | 42 317 | 42 167 | 30 665 | 0.104 | 0.093 |

^a The weighted least squares R factor on intensity for symmetry-related observations: $R_w = \mathbf{S}[(I_i - G_{ij} \langle I_j \rangle / s_{ij})^2 / \mathbf{S}(I_{ij}/s_{ij})^2]$, where $G_{ij} = g_i + A_i s_j + B_i s_j^2$; $s = \sin \theta / \lambda$; A and B are scaling parameters. ^b The unweighted absolute R factor on intensities: $R_{uw} = \mathbf{S}(I_{ij} - G_{ij} \langle I_j \rangle / \mathbf{S}(I_{ij}))$.

in *total* surface areas between the various conformations of hemoglobin are only a few percent. Therefore, they are not meaningful because of the different effect of crystal packing and crystallographic errors on the position of the surface side chains. Nevertheless, differences in surface areas as a result of the presence or absence of the linker are well determined and are the quantities we are concerned with.

Crystallographic Analyses. (A) *Protein Crystallization.* Crystals of deoxy-HbA and deoxy-DecHb were obtained by adapting a procedure described by Perutz (1968), namely, 2.5 M ammonium phosphate at pH 6.5 and a protein concentration of 1 g/dL. All solutions were stored under nitrogen. Single crystals measuring more than 0.7 mm in their largest dimension grew after several weeks.

(B) *X-ray Data Collection and Data Processing.* The data crystal with the dimensions of $0.8 \times 1.0 \times 1.0$ mm³ was mounted in a thin-walled capillary tube with the diameter of 1.5 mm. X-ray diffraction data were collected using a Siemens electronic area detector positioned 10 cm away from the data crystal. The area detector was mounted on a three-axis Supper oscillation camera controlled by a PCS microcomputer. Each electronic frame was composed of counts summed over a 0.25° range in ω with exposure times of 120 s. The individual frames were contiguous in that the beginning of each angular range in ω coincided with the end of the previous range. The raw data frames were transferred from the PCS microcomputer to a Silicon Graphics Indigo 2 computer for final processing. The data collection was carried out at controlled room temperature (19–20 °C). The raw data frames were processed with the XENGEN program system (Howard et al., 1987). The total observations up to the resolution of 1.9 Å were 108 860. The number of unique reflections was 42 167 (99.6% of the crystallographically possible reflections). Detailed statistics for the X-ray diffraction data are given in Table 1.

Measurements of Oxygen Affinity. These measurements were performed using the thin-layer Gill's cell (Dolman & Gill, 1978). Numerical analyses were based on the binding polynomial (Wyman & Gill, 1990)

$$P = 1 + \beta_1 X + \beta_2 X^2 + \beta_3 X^3 + \beta_4 X^4 \quad (1)$$

where the overall Adair's constants, β_i 's, are related to the intrinsic statistical affinity constants, K_i 's, of the subsequent steps of oxygenation by $\beta_i = C_{4,i} K_i \dots$ ($i = 1-4$), where $C_{4,i}$ is the binomial coefficient $4!/i!(4-i)!$. The quantity X is the observed partial pressure of oxygen, P_{O_2} . Using the binding polynomial (Wyman & Gill, 1990), we have

$$y = d \ln P / 4 d \ln(P_{O_2}) \quad (2)$$

where y is the fractional saturation of hemoglobin with oxygen.

The stepwise difference data obtained with the Gill's cell were analyzed using

$$\Delta OD_i = \Delta OD_T \times \Delta y \quad (3)$$

where ΔOD_i is the optical density change at each dilution step, Δy is the corresponding change of the fractional saturation, and ΔOD_T is the total optical density change upon complete saturation–desaturation with oxygen.

The binding isotherms were measured at pH 9.0 in 0.1 M borate buffer because under these conditions the Bohr effect of hemoglobin is finished and at alkaline pH the interaction with anions is minimized. This allowed a comparison of the functional characteristics of HbA and DecHb.

Following a procedure previously described, global analyses of six isotherms obtained at temperatures between 15 and 40 °C were used for recovering the standard β_i 's parameters at 25 °C. The median ligand activity was computed from $P_m = \beta_4^{-0.25}$ (Wyman & Gill, 1990).

RESULTS

Purification and Characterization of DecHb. Repetitive chromatographies are used to isolate pure samples of β - β cross-linked DecHbA. The preparation is accepted only when reversed phase chromatography (Bucci et al., 1993) indicates the presence of only two protein fractions: the unmodified α and the cross-linked β subunits, respectively. These analyses prove that the used samples have a purity of 99% or better. The cross-linked nature of the β subunits recovered from reversed-phase chromatography is demonstrated by SDS–PAGE electrophoresis where a single band appears with the mobility of a 32 kDa polypeptide. The cross-link is proven to be intramolecular by sedimentation velocity experiments performed on 2 and 4 mg/mL samples, respectively. The Schlieren images show the presence of two isolated symmetrical peaks with $s_{20,w} = 4.45$ and 4.26, respectively, as expected from the concentration dependence of the sedimentation velocity of a tetrameric hemoglobin.

Tryptic peptide maps (Figure 2) are obtained as previously described (Bucci et al., 1993). In the cross-linked β subunits they show the absence of peptides 9 and 10 and the appearance of a new combined peptide 9 + 10. Inspection of Table 2 indicates that this results from the chemical substitution of the β 82 lysine, positioned at the end of peptide 9, which prevents the tryptic cleavage of peptides 9 and 10. This was confirmed by sequencing the combined peptide 9 + 10. These analyses confirm that the sebacyl residue bridges the two β 82 lysines of the partner subunits across

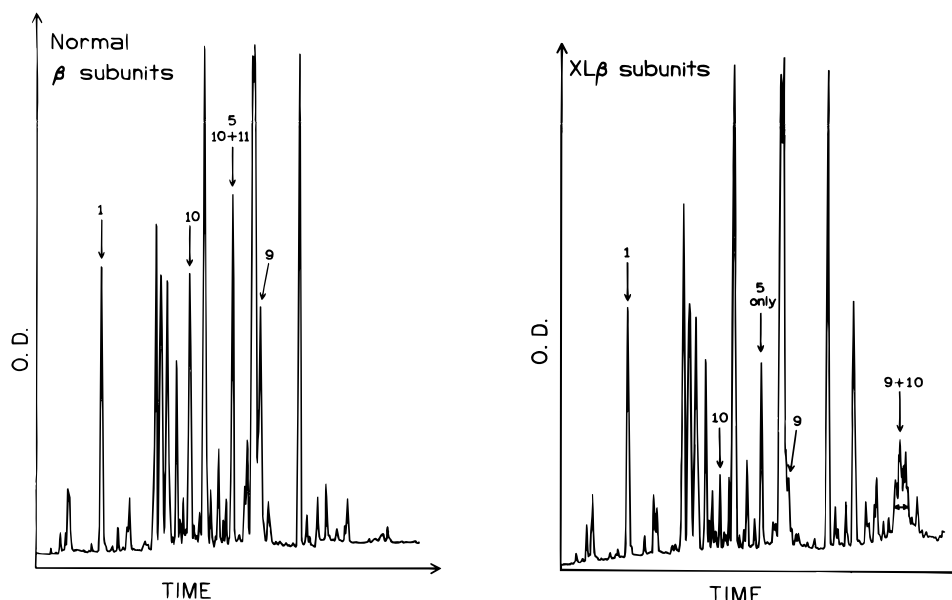


FIGURE 2: Tryptic peptide maps of normal and cross-linked β subunits. Notice the disappearance of peptides 9 and 10 in XL β where a new peptide appears which is the combination of peptides 9 and 10. The amino acid sequence of the 9 + 10 peptide confirms the chemical substitution of the lysine at β 82.

Table 2: Tryptic Fragments of Human Hemoglobin β -Chain

| fragment | residues | sequence |
|----------|----------|---------------------|
| 01 | 1–8 | VHLTPEEK |
| 02 | 9–17 | SAVTALWGK |
| 03 | 18–30 | VNVDEVGGEALGR |
| 04 | 31–40 | LLVVYPWTQR |
| 05 | 41–59 | FFESFGDLSTPDVVMGNPK |
| 06 | 60–61 | VK |
| 07 | 62–65 | AHGK |
| 08 | 66 | K |
| 09 | 67–82 | VLGAFSDGLAHLNLIK |
| 10 | 83–95 | GTATLSELHCDK |
| 11 | 96–104 | LHVDPENFR |
| 12 | 105–120 | LLGNVLVCVLAHHFGK |
| 13 | 121–132 | EFTPPVQAAYQK |
| 14 | 133–144 | VVAGVANALAHK |
| 15 | 145–146 | YH |

the β -cleft of hemoglobin. Peptide maps of the α chains of DechHb did not reveal any other modification of the protein.

Crystallographic Refinement. The starting model for the refinement of cross-linked human deoxyhemoglobin was the 2.2 Å resolution model of the wild-type human deoxyhemoglobin (Fronticelli et al., 1994) after the deletion of 2 sulfate anions and all 464 water molecules. The refinement was performed on a CRAY Y-MP computer with GPRLSA (Furey et al., 1982) and the restrained least squares refinement procedure of Hendrickson and Konner (1980a,b) and Hendrickson (1985a,b). The algorithm O (Jones et al., 1991; Kones & Kjeldgaard, 1993) was used on a Silicon Graphics, Inc., Indigo 2 computer with a GR3-XZ graphics system for examining the $2F_o - F_c$, $F_o - F_c$, and omit maps, for adjusting the protein atoms, and for adding solvent molecules.

Periodically, during the refinement procedure, the entire model was checked and adjusted to conform to the electron density maps. Water molecules and sulfate anions were located in the different Fourier maps as peaks higher than 3σ . After all the possible solvent molecules were found, they were verified by a series of omit maps (Furey, 1990). This procedure was performed in ascending order starting from the bottom of the list of water molecules, ranked

Table 3: Summary of Least Squares Refinement Parameters for Cross-Linked Human Deoxyhemoglobin

| | target values | final model |
|--|---------------|-------------|
| diffraction data ^a from 6.0 to 1.9 Å with $I \geq 1\sigma(I)$ | | 33545 |
| crystallographic R^b factor | | 0.172 |
| no. of residues | | 578 |
| no. of water molecules | | 393 |
| no. of non-H protein atoms/water molecules | | 11.2 |
| RMS deviations from ideal distances (Å) | | |
| bond distances | 0.020 | 0.017 |
| angle distances | 0.036 | 0.037 |
| planar 1–4 distances | 0.040 | 0.042 |
| RMS deviations from planarity (Å) | 0.030 | 0.023 |
| RMS deviations from ideal chirality (Å ³) | 0.200 | 0.206 |
| thermal parameter correlation (mean/DB) | | |
| main-chain bond | 1.000 | 0.794 |
| main-chain angle | 1.500 | 1.237 |
| side-chain bond | 1.500 | 1.628 |
| side-chain angle | 2.000 | 2.431 |

^a Data used for least squares refinement. All data were used in the calculation of electron density maps. ^b The crystallographic $R = \sum_{hkl} ||F_o| - |F_c|| / \sum_{hkl} |F_o|$.

according to the parameter OCC^2/B (James & Sielecki, 1983), the ratio of the square of the fractional occupancy factor (OCC) of the oxygen atom position and the crystallographic temperature factor (B). Lower resolution diffraction data, excluded from the refinement, were included in all map calculations. The current crystallographic R factor was 0.172 for data between 6.0 and 1.9 Å resolution. A summary of the crystallographic refinement is found in Table 3. The final coordinates for the structure of cross-linked human deoxyhemoglobin have been deposited in the Brookhaven Protein Data Bank (Bernstein et al., 1977).

The atomic structure of deoxy-DechHb is similar to that of the unliganded normal HbA (Fermi et al., 1984; Fronticelli et al., 1994). The $2F_o - F_c$ electron density map shown in Figure 3 reveals complete density for both of the β 82 lysines and the presence of electron density of the sebacyl residue that spans the β -cleft. Breaks occur in the electron density between the sebacyl and the lysine residues, suggesting that

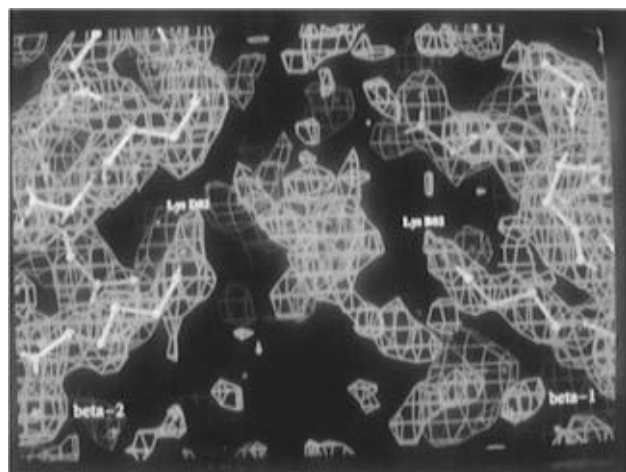


FIGURE 3: $2F_o - F_c$ electron density map of the β -cleft of deoxy-DecHb contoured at 0.5σ . The central body is the cross-linking bridge between the two $\beta 82$ lysines.

the sebacyl may have several conformations. The model used in the refinement does not include atoms for the sebacyl residue, and thus the electron density in the β -cleft is unbiased.

Molecular Modeling. Lysine $\beta 82$ is situated on the F helix. In the T (Fronticelli et al., 1994; Fermi et al., 1984), R (Shanaa, 1983), and R₂ (Silva et al., 1992) crystal structures the C_α - C_β bond points into the 2,3-DPG binding pocket, on the side of the helix forming part of the cleft lining. In all three conformational forms, the side chains have high temperature factors, indicating that they are very mobile and that therefore the reported crystallographic positions probably represent one of many approximately equienergetic side-chain conformations. In all three conformations, the side chains are reported to lie inside the cleft rather than to protrude out into bulk solution. The crystal structure for the T form of DecHb also has high temperature factors for the lysine side chains and discontinuous density for the linker. This cross-linked structure establishes that, in the T form, the rest of the protein molecule is essentially unaffected by the presence of the linker. In all the crystal structures, the backbone around position $\beta 82$ has low temperature factors, indicating a high degree of ordering.

A single linker conformation was built into each of the T, R, and R₂ crystal structures. On the basis of the above observations, it was assumed that the lysine side chains will change conformation somewhat to adapt to the presence of the linker but that the conformation of the rest of the protein molecule is unaltered in all cases. Thus, the conformational variables for the modeling are the χ_1 , χ_2 , and χ_3 angles of both lysine side chains and the nine single torsion angles within the linker. With these degrees of freedom, multiple conformations are possible in all three protein conformations. No attempt was made to systematically survey these. Rather, one subjectively representative conformation was selected and a visual inspection made of the possible alternatives. Coordinates of the cross-linked models are available on the Internet via anonymous ftp from iris4.carb.nist.gov, directory pub/hb-models.

The fully extended linker is approximately 14 Å long between the positions that would represent the NZ atoms of the lysines. With extended lysine side chains added, it could

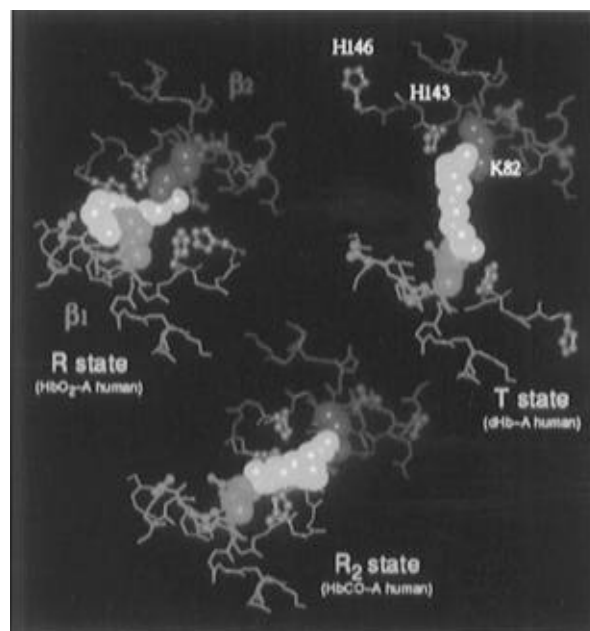


FIGURE 4: Modeled insertion of the linker sebacyl residue (yellow) between the $\beta 82$ lysines of the partner β subunits (red and green) in the T, R, and R₂ structures of hemoglobin. Note the position of the imidazole residues (blue) of histidines $\beta 143$ and $\beta 146$. They point away from the linker in the T structure, while in R and R₂ they move close to the linker, severely limiting the conformational freedom of the system.

in principle link C_α atoms up to about 26 Å apart. In the T, R, and R₂ structures the $\beta 82$ C_α distances are 19.5, 14.9, and 17.2 Å, respectively.

In the deoxy (T) (Fronticelli et al., 1994; Fermi et al., 1984) conformation the linker can fit comfortably into the open 2,3DPG binding pocket, and many alternative conformations of the lysine side chains and linker appear possible (Figure 3). The chosen conformation moves the NZ atoms of the lysine side chains by 1 and 2 Å from the unliganded structure and positions the linker bowing away from the floor of the pocket. All the possible conformations of the linker appear highly exposed to solvent because of the open nature of the pocket and the fairly extended conformations needed to bridge between the lysines. The chosen conformation is one of the most exposed possible. The model was built before the crystal structure was available. Comparison of the model and the experiment shows the linker to follow a path further from the floor of the β -cleft than is indicated by the disjointed electron density in the crystallographic map.

In the R crystal structure (Shanaa, 1983), the distance between the $\beta 82$ lysine C_α atoms is about 4.5 Å shorter than in the deoxy structure, and the $\beta 82$ side chains are folded back against the wall of the pocket, making the NZ atoms inaccessible for attachment to the linker. Difficulty is experienced in finding any position of the side chains which allow the linker to be accommodated, partly because of the need to move the side chains away from the cleft wall, partly because of the narrowness of the cleft, and partly because of steric clashes with the imidazole side chains of histidines $\beta 143$ and $\beta 146$. The selected conformation has an asymmetric arrangement of the lysine side chains and a very bent conformation of the linker (Figure 4). As a result of these features, the linker is much less exposed to solvent than in the T-state model and appears to have much less conformational freedom.

Table 4: Overall Adair's Constants (β_i) and Resulting Intrinsic Affinity Constants (K_i) for the Subsequent Steps of Oxygenation of Normal Human Hemoglobin and DecHb^a

| protein | β_1 (torr ⁻¹) | β_2 (torr ⁻²) | β_3 (torr ⁻³) | β_4 (torr ⁻⁴) |
|-----------|---------------------------------|---------------------------------|---------------------------------|---------------------------------|
| normal Hb | 0.859 | 0.469 | 0.214 | 0.263 |
| DecHb | 0.860 | 0.011 | 0.021 | 0.008 |
| | K_1 (mM ⁻¹) | K_2 (mM ⁻¹) | K_3 (mM ⁻¹) | K_4 (mM ⁻¹) |
| normal Hb | 139.4 | 235.9 | 445.5 | 3193.2 |
| DecHb | 139.7 | 5.4 | 1930.6 | 1024.7 |

^aThe values of the β_1 constants at 25 °C (here presented) were estimated from simultaneous analyses of six isotherms obtained at different temperatures between 15 and 40 °C in 0.1 M borate buffer at pH 9.0. The standard deviation of the recovered parameters was less than 1% of the estimated values.

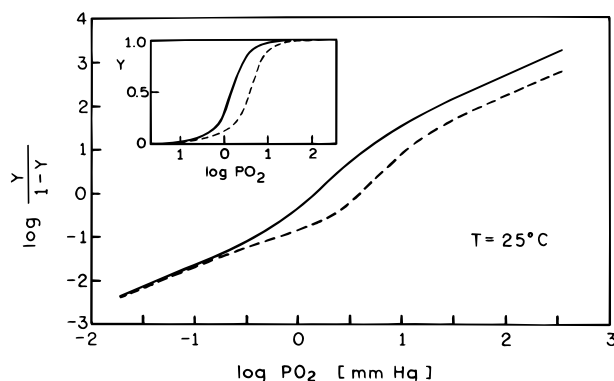


FIGURE 5: Hill plots for normal hemoglobin (continuous line) and DecHb (dashed line) computed from the overall Adair's constants in Table 4. The two curves clearly indicate the very similar oxygen affinities of the respective T states, while the intermediates of oxygenation and the final fully liganded state of DecHb have a lower oxygen affinity than that of normal hemoglobin. The inset shows the isotherms of the two proteins. Data at 25 °C recovered from global analyses performed in 0.1 M borate buffer at pH 9.0, at temperatures between 15 and 40 °C.

In the R2 structure (Silva et al., 1992), the distance between the residue β 82 backbone positions is slightly larger than in R, so that the linker can be more easily accommodated with only moderate bending. However, in this structure, the histidines at β 143 and 146 from the two subunits are close together, leaving a narrow gully between them for the linker to pass through (Figure 4).

Oxygen Affinity Characteristics. The standard Adair's parameters for DecHb at 25 °C recovered from the global analyses of six isotherms at different temperatures between 15 and 40 °C are shown in Table 4. These parameters were used to compute the Hill's plots shown in Figure 5 and the isotherms in the inset. They show a distinct right shift of the binding isotherm of DecHb. The p_m values are 8.4 and 4.2 for DecHb and HbA, respectively.

There is a substantial difference between the intrinsic affinity constants, K_i , of HbA and DecHb. In HbA the constants increase by approximately 2-fold at each step except for the fourth step where the increase is 7-fold over the affinity of the third step. In DecHb the first step has the same affinity as in HbA; then the two systems diverge. The affinity of the second step of oxygenation of DecHb is 27 times lower than that of the first step, the third step-affinity is 360 times higher than that of the second, and the last affinity at the fourth step is twice lower than that of the third. This indicates the presence of both negative and positive cooperativities in the intermediates of oxygenation.

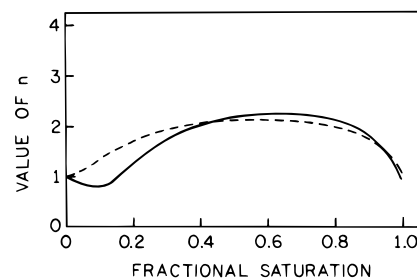


FIGURE 6: Dependence of the slope of the Hill plots (i.e., Hill's parameter n) on the fractional saturation of DecHb (continuous line) and natural HbA. Note the slope lower than 1 near 10% saturation for DecHb.

As shown in Figure 6, the maximum value of cooperativity is reached in both cases between 60% and 70% saturation, where the values of the Hill's parameter n are 2.2 and 2.0 for DecHb and HbA, respectively. Also, the curve for DecHb shows the presence of a distinct negative cooperativity near the 10% saturation, with the value of n falling from $n = 1$ to $n = 0.8$. This is due to the decreased oxygen affinity of the second step. Notably, the maximum value of n is higher in the cross-linked system, due to the large increase of the affinity of the third step of oxygenation.

DISCUSSION

Factors Affecting Oxygen Affinity. As reported, under our conditions, DecHb has a p_m distinctly lower than that of HbA, 8.4 and 4.2 mmHg, respectively. The atomic coordinates of deoxy-DecHb crystals are very similar to those of the T form of HbA (Fronticelli et al., 1994; Fermi et al., 1984). The intrinsic Adair's constants of the first oxygenation step of DecHb and HbA are also very similar (Table 4). This indicates that the unliganded forms of DecHb and HbA are almost identical in structure and function. The Hill plots in Figure 5 and the intrinsic constants in Table 4 confirm that the linker affects only the partially and fully liganded forms of the system. It appears that the liganded forms of DecHb are responsible for regulating the overall oxygen affinity of the molecule to a lower level than in HbA.

The relative stabilization of the different conformations of the hemoglobin tetramer by the cross-link appears to be predominantly determined by five factors:

(1) **Steric Crowding.** While modeling suggests that the T and R2 conformations can accommodate the 10 carbon long linker, it appears to be severely restricted in the R conformation. It is not known at the present time whether the R or the R2 or some other states closely resemble the physiologically relevant oxy conformation of the molecule. Structural analysis (Srinivasan & Rose, 1994; Janin & Wodak, 1993) suggests that R is an intermediate structure between T and R2. It is thus possible that there may be other intermediates near to the R conformation that are unable to accommodate the linker without substantial steric strain. Such conformations would be heavily destabilized by the linker.

(2) **Burial of Nonpolar Area.** The hydrophobic effect is thought to be closely coupled to the amount of nonpolar area exposed to solvent. Comparing the change in nonpolar surface area for the T to R and the T to R2 transitions of the native and modeled cross-link structures (Table 5), we find that the linker produces an extra burial of approximately 250 Å² in nonpolar area going from T to either R or R2. Applying a conservative free energy estimate of 83 J/Å² (20

Table 5: Increase in Burial of Polar and Nonpolar Surface Areas in the Presence of the Sebacyl Linker for Known Conformational Transitions of Human Hemoglobin ($\text{\AA}^2/\text{mol}$ of tetramer)^a

| T \rightarrow R | | | T \rightarrow R2 | | | R \rightarrow R2 | | |
|-------------------|----------|-------|--------------------|----------|-------|--------------------|----------|-------|
| polar | nonpolar | total | polar | nonpolar | total | polar | nonpolar | total |
| 26 | 243 | 269 | -70 | 253 | 182 | -96 | 9 | 87 |

^a Areas are based on approximate models of the linker (see text). A positive burial change implies increased stability of the system after the transition.

cal/ \AA^2) of buried hydrophobic area, this corresponds to an upper limit of about 21 kJ/mol of tetramer (5kcal/tetramer) favoring the liganded conformations.

(3) *Burial of Polar and Charged Groups.* The area calculations indicate a substantial uncompensated desolvation of polar and charged groups in the 2,3DPG binding pocket upon introducing the cross-link in all states. However, the area changes accompanying the conformational transitions are relatively small, particularly for T \rightarrow R (Table 5), so that relative stabilities are little affected.

(4) *Configurational Entropy.* Modeling suggests that many more linker conformations are possible in the T state than in the R2 and R conformations. The associated free energy advantage arising from such conformational entropy effects favors the T state. The formal upper limit for this contribution of about 38 kJ/mol of tetramer (9 kcal/tetramer; 1 kcal/mol per single bond) is significantly reduced by the conformational restrictions of the linker already present in the T state.

(5) *Internal Mobility.* Mobility changes in the hemoglobin molecule for the different conformations caused by the cross-link may also affect oxygen affinity. None of the observed crystal structures have access channels to the heme pocket large enough to allow oxygen to pass in and out. Consequently, channels opened by thermal motion involving nonequilibrium conformations must determine the on and off rates of oxygen binding. At any stage of oxygenation, the sebacyl cross-link may thus affect on rates and off rates differently, resulting in changed oxygen binding constants.

The overall free energy balance favoring one conformation or another is a delicate balance between these factors and cannot be even approximately calculated. The most important information obtained from the modeling is that the degree of conformational freedom of liganded DecHb is severely limited, much more than in its unliganded form. This is strongly reflected in the experimental efficiency of the cross-linking procedure: When the cross-linking is performed on deoxyhemoglobin, more than 80% of hemoglobin is specifically cross-linked. In contrast, when liganded hemoglobin is used for chemical treatment, only a small fraction of the protein reacts into a largely heterogeneous mixture, which may include, but from which it is difficult to extract, the $\beta_1\text{82}-\beta_2\text{82}$ cross-linked DecHb.

Possible Allosteric Models. Inspection of Table 4 clearly shows that the first step of oxygenation had very similar intrinsic affinity in both HbA and DecHb, confirming the crystallographic and modeling evidence. The difference between the two proteins starts with the second step of oxygenation in which the affinity is 50 times lower than that of the corresponding step in HbA and, most importantly, 27 times lower than the affinity of its first step.

Clearly, in DecHb there is a negative binding cooperativity between the first and second step of oxygenation. The system loses affinity and the Hill parameter "*n*" at low fractional saturations becomes lower than 1.0 (Figure 5). It has been proposed that the α subunits are the first to be saturated with ligands (Abraham et al., 1992). This implies that in DecHb there is a strong negative interaction between the first saturated α subunit heme and all other hemes.

In DecHb, the third step has an intrinsic oxygen affinity 360 times higher than that of the second step, indicating a very strong binding cooperativity. It produces a value of $n = 2.2$ in the Hill plot. The fourth step has an affinity two times lower than the third step. This again indicates a negative cooperativity, although it is too low to be detected in the Hill plot. Thus, it appears that the oxygen binding properties of DecHb are regulated by successive steps of positive and negative binding cooperativities.

Searching for an allosteric model, the MWC model must be excluded because it cannot explain negative cooperativities. The KNF model is also excluded. It can explain negative cooperativities but not an alternate succession of positive and negative cooperativities. Models restricted to a minimum number of conformational events do not fit the data for DecHb, which seems to be a multistate system, where each intermediate of oxygenation has its own conformation, some with high and some with low oxygen affinity.

It is interesting to note that negative cooperativity of intermediates can still produce a distinct overall positive cooperativity, as anticipated by DiCera (1990). The question may be posed whether this is a peculiarity of DecHb produced by the cross-linking of the β subunits, with no correlation with the allosteric properties of HbA.

Under the present conditions, at pH 9.0 in 0.1 M borate buffer, HbA does not show negative cooperativities. However, they cannot be excluded from the system. At neutral pH, and in the presence of chloride ions, the third step of oxygenation becomes so low that the overall Adair's constant β_3 is very close to 0.0. This led Johnson et al. (1992) to propose that HbA has a very low oxygen affinity, i.e., a negative cooperativity, at the third oxygen binding step. If this hypothesis is correct, the main effect of the cross-link in DecHb would be to displace that phenomenon from the third to the second step of oxygenation.

In a similar fashion, the "quaternary enhancement" (Ackers et al., 1992) is represented in HbA by a 7-fold increased affinity at the fourth oxygenation step and in DecHb by a 360-fold increase of the affinity at the third step.

A multistate system for HbA, where the intermediates have their own conformation, is supported by several lines of evidence including cryoelectrophoresis (Perrella et al., 1990) and Raman spectroscopy (Jayaraman & Spiro, 1995). It receives the strongest support from the "erratic" behavior of the enthalpies at the subsequent steps of oxygenation, which alternate from positive to excessively negative values (Bucci et al., 1991; Johnson et al., 1992).

Before the surfacing of the data mentioned above and those reported here, it appeared that the form presiding over the allosteric regulations of the system was the T, deoxygenated, structure. In fact, it is the form which is stabilized by and binds the anions, polyanions, and proton effectors, which decrease the oxygen affinity of hemoglobin. Conversely, the T conformation disappears from the system when

mutations increase the oxygen affinity by locking hemoglobin into its oxy structure. Now it appears that a strong regulatory power is linked to the polymorphism of the partially and fully liganded forms.

We cannot assess experimentally whether there is conservation of conformational species between the liganded forms of HbA and DecHb. In view of the variety of liganded forms recently identified, it is reasonable to propose that the linker only stabilizes conformations that are always accessible to HbA, though in much lower fractions. As discussed above, the low conformational freedom of the liganded states in DecHb would justify a different conformational distribution of the intermediates of oxygenation. Thus, the difference between HbA and DecHb would essentially be the distributions of molecular species at the various oxygenation steps, of which we detect average characteristics.

REFERENCES

- Abraham, D. J., Peascoe, R. A., Randad, R. S., & Panikker, J. (1992) *J. Mol. Biol.* 227, 480–492.
- Ackers, G. K., Doyle, M. L., Myers, D., & Daugherty, M. (1992) *Science* 255, 54–63.
- Bernstein, F. C., Koetzle, T. F., Williams, G. J. B., Meyer, E. F., Jr., Brice, M. D., Rogers, J. R., Kennard, O., Shimanouchi, T., & Tasumi, M. (1977) *J. Mol. Biol.* 112, 535–542.
- Bucci, E., & Fronticelli, C. (1994) U.S. Patent 5290919.
- Bucci, E., & Fronticelli, C. (1995) U.S. Patent 5387672.
- Bucci, E., Malak, H., Fronticelli, C., Gryczynski, I., & Lakowicz, J. R. (1988) *J. Biol. Chem.* 263, 6972–6977.
- Bucci, E., Fronticelli, C., & Gryczynski, Z. (1991) *Biochemistry* 30, 3195–3199.
- Bucci, E., Fronticelli, C., Gryczynski, Z., Razynska, A., & Collins, J. H. (1993) *Biochemistry* 32, 3519–3526.
- Bucci, E., Razynska, A., Kwansa, H., & Fronticelli, C. (1994) 11th Congress of the International Society for Artificial Cells, Blood Substitutes and Immobilization Biotechnology Boston, MA, July.
- Chothia, C. (1976) *J. Mol. Biol.* 105, 1–14.
- DiCera, E. (1990) *Biophys. Chem.* 37, 147–164.
- DiCera, E., Robert, C. H., & Gill, S. J. (1987) *Biochemistry* 26, 4003–4008.
- Dolman, D., & Gill, S. J. (1978) *Anal. Biochem.* 87, 127–134.
- Fermi, G., Perutz, M. F., Shaanan, B., & Forume, R. (1984) *J. Mol. Biol.* 175, 159–174.
- Fronticelli, C., Pechik, I., Brinigar, W. S., Kowalczyk, L., & Gilliland, G. L. (1994) *J. Biol. Chem.* 269, 23965–69.
- Furey, W. (1990) *Abstracts of the American Crystallographic Association Fortieth Anniversary Meeting*, New Orleans, LA, PA33.
- Furey, W., Wang, B. C., & Sax, M. (1982) *J. Appl. Crystallogr.* 15, 160–166.
- Gill, S. J., Robert, C. H., Coletta, M., DiCera, E., & Brunori, M. (1986) *Biophys. J.* 50, 747–752.
- Hendrickson, W. (1985a) *Methods Enzymol.* 115, 252–270.
- Hendrickson, W. (1985b) in *Crystallographic Computing 3: Data Collection, Structure Determination, Proteins, and Databases* (Sheldrick, G., Kruger, C., & Goddard, R., Eds.) pp 306–311, Clarendon Press, Oxford.
- Hendrickson, W., & Konnert, J. (1980a) in *Computing in Crystallography* (Diamond, R., Ramaseshan, S., & Venkatesan, K., Eds.) pp 1301–1323, Indian Academy of Sciences, Bangalore.
- Hendrickson, W., & Konnert, J. (1980b) in *Biomolecular Structure, Function, Conformation and Evolution* (Srinivasan, R., Ed.) Vol. 1, pp 43–57, Pergamon, Oxford.
- Howard, A. J., Gilliland, G. L., Finzel, B. C., Poulos, T. L., Ohlendorf, D. H., & Salemme, F. R. (1987) *J. Appl. Crystallogr.* 20, 383–387.
- James, M. N. G., & Sielecki, A. R. (1983) *J. Mol. Biol.* 163, 299–361.
- Janin, J., & Wodak, S. J. (1993) *Proteins: Struct. Funct. Genet.* 15, 1–4.
- Jayaraman, V., & Spiro, T. G. (1995) *Biochemistry* 34, 4511–4515.
- Johnson, C. R., Ownby, D. W., Gill, S. J., & Peters, K. S. (1992) *Biochemistry* 31, 10074–10082.
- Jones, T. A., & Kjeldgaard, M. (1993) *O Version 5.9.1*, Department of Molecular Biology, BMC, Uppsala University, Sweden, and Department of Chemistry, Aarhus University, Denmark.
- Jones, T. A., Zou, J.-Y., Cowan, S. W., & Kjeldgaard, M. (1991) *Acta Crystallogr. A* 47, 110–119.
- Jones, R. T., Head, C. G., Fujita, T. S., & Shih, D. T. (1993) *Biochemistry* 32, 215–223.
- Kluger, R., Wodzinska, J., Jones, R. T., Head, C. G., Fujita, T. S., & Shih, D. T. (1992) *Biochemistry* 31, 7551–7559.
- Koshland, D. E., Jr., Nemethy, G., & Filmer, D. (1966) *Biochemistry* 5, 365–385.
- Lee, B., & Richards, F. M. (1971) *J. Mol. Biol.* 55, 379–400.
- Monod, J., Wyman, J., & Changeux, J. P. (1965) *J. Mol. Biol.* 12, 88–118.
- Mosimann, S., Meleshko, R., & James, N. M. G. (1995) *Proteins* 23, 301–317.
- Perrella, M., Benazzi, L., Shea, M. A., & Ackers, G. K. (1990) *Biophysical Chemistry* 35, 97–103.
- Perutz, M. F. (1968) *J. Cryst. Growth* 2, 54–55.
- Razynska, A., Rak, J., Fronticelli, C., & Bucci, E. (1991) *J. Chem. Soc., Perkin Trans. 2*, 1531–1540.
- Schumacher, M. A., Dixon, M. M., Kluger, R., Jones, R. T., & Brennan, R. G. (1995) *Nature* 375, 84–87.
- Shaanan, B. (1983) *J. Mol. Biol.* 171, 31–59.
- Silva, M. M., Rogers, P., & Arnone, A. (1992) *J. Biol. Chem.* 267, 17248–17256.
- Smith, F. R., Lattman, E. E., & Carter, C. W. (1991) *Proteins* 10, 81–91.
- Srinivasan, R., & Rose, G. D. (1994) *Proc. Natl. Acad. Sci. U.S.A.* 91, 11113–11117.
- Wyman, J., & Gill, S. J. (1990) *Binding and linkage*, University Science Books, Mill Valley, CA.